Competition between Pairing and Ferromagnetic Instabilities in Ultracold Fermi Gases near Feshbach Resonances

David Pekker,[1] Mehrtash Babadi,[1] Rajdeep Sensarma,[2] Nikolaj Zinner,[1,3] Lode Pollet,[1] Martin W. Zwierlein,[4] and Eugene Demler[1]

[1]*Physics Department, Harvard University, Cambridge, Massachusetts 02138, USA*
[2]*Condensed Matter Theory Center, University of Maryland, College Park, Maryland 20742, USA*
[3]*Department of Physics and Astronomy, Aarhus University, Aarhus, DK-8000, Denmark*
[4]*MIT-Harvard Center for Ultracold Atoms, Research Laboratory of Electronics, and Department of Physics, Cambridge, Massachusetts 02139, USA*

(Received 26 May 2010; revised manuscript received 31 December 2010; published 1 February 2011)

We study the quench dynamics of a two-component ultracold Fermi gas from the weak into the strong interaction regime, where the short time dynamics are governed by the exponential growth rate of unstable collective modes. We obtain an effective interaction that takes into account both Pauli blocking and the energy dependence of the scattering amplitude near a Feshbach resonance. Using this interaction we analyze the competing instabilities towards Stoner ferromagnetism and pairing.

DOI: 10.1103/PhysRevLett.106.050402 PACS numbers: 05.30.Fk, 03.75.Ss, 67.85.−d

Ferromagnetism in itinerant fermions is a prime example of a strongly interacting system. Most theoretical treatments rely on a mean-field Stoner criterion [1], but whether this argument applies beyond mean-field remains an open problem. It is known that the existence of the Stoner instability is very sensitive to the details of band structure and interactions [2–4]. However, how to account for these details in realistic systems remains poorly understood. Following theoretical proposals [5], the MIT group made use of the tunability [6] and slow time scales [7–10] of ultracold atomic systems to study the Stoner instability [11]. Signatures compatible with ferromagnetism, as understood from mean-field theory [12], were observed in experiments: a maximum in cloud size, a minimum in kinetic energy and a maximum in atomic losses at the transition. However, no magnetic domains were resolved.

An important aspect of the MIT experiments is that the Fermi gas was prepared with weak interactions after which the interactions were ramped to the strongly repulsive regime. Dynamic rather than adiabatic preparation was used to avoid production of molecules. This raises the question of what are the dominant instabilities of the Fermi gas in the vicinity of a Feshbach resonance.

Naively, one expects that on the BEC side, molecule production is slow, as it requires a three-body process. Therefore, the instability towards Stoner ferromagnetism should dominate over the instability toward molecule production. Likewise, one expects that quenches to the attractive (BCS) side always yield a pairing instability.

In this Letter, we argue that this picture, which was used to interpret the MIT experiments, is incomplete. Near the Feshbach resonance, even on the BEC side, pair production remains a fast two-body process as long as the Fermi sea can absorb the molecular binding energy. As a result, near the Feshbach resonance, both on the BEC and the BCS side, the pairing and the Stoner instabilities compete.

We start by describing the interatomic interactions. A Feshbach resonance enables tunable interactions between ultracold atoms by coupling the collision partners to a molecular state with a different magnetic moment. For broad resonances, where the coupling is much larger than the Fermi energy, this can be modeled by a single collision channel that supports one shallow bound state [13]. An often used, but pathological choice, is the hard-sphere pseudopotential. Although at low energies the scattering amplitude from the hard-sphere potential and the T matrix match, at higher energies comparable to the molecular binding energy, they do not [14]. In the strong interaction Stoner-regime, the Fermi energy is comparable to the binding energy of a molecule in vacuum, precluding the use of the hard-sphere potential.

In light of this remark, we study the initial dynamics of the collective modes of a fermionic system after a sudden quench, taking the Cooperon (full T matrix and Pauli blocking) into account. We focus on the case of a sudden quench, as it is simpler and captures the essential physics of the instability of the Fermi surface. Our main findings are summarized in Fig. 1 and are: (a) With the full T matrix the Stoner instability survives with a finite growth rate in the range $-0.2 \lesssim k_F a \lesssim 1$, where a is the scattering length and k_F the Fermi momentum. In contrast, bare interactions [15] result in an unphysical divergence of the growth rate at unitarity and no magnetic instabilities on the BCS side (see Fig. 1). (b) The pairing instability persists on the BEC side, where it competes with the Stoner instability. (c) The pairing instability is always stronger.

Pairing and Stoner instabilities on the wrong side of the resonance seem remarkable. Both can be understood by

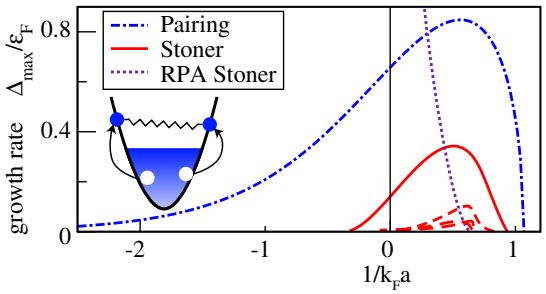

FIG. 1 (color online). Growth rate of the pairing and Stoner ferromagnetic instabilities after a quench as a function of the final interaction strength $1/k_Fa$. Final interactions with negative (positive) values of $1/k_Fa$ correspond to the BCS (BEC) side of the Feshbach resonance. The Stoner instability simultaneously occurs in multiple channels. The most unstable channel is indicated by the solid red line, the others by dashed red lines. The "RPA Stoner" instability corresponds to the RPA result with bare interactions (see text and Ref. [15]). Inset: Schematic diagram of the pair creation process showing the binding energy (spring) being absorbed by the Fermi sea (arrows).

taking into account the Fermi sea. On the BEC side, due to Pauli blocking, the binding energy of the pairlike molecule can be absorbed by the two holes that are left behind (see the inset of Fig. 1). Thus, the two-body pairing process becomes forbidden when the binding energy $\sim 1/ma^2$ exceeds the maximum energy that can be absorbed by the holes $\sim k_F^2/m$ (m is the fermion mass, and in which $\hbar = 1$). On the BCS side, although interactions at low energies are indeed attractive, the same is not true at high energies. As the Stoner instability involves all scattering energies up to the Fermi energy, it can persist on the BCS side.

Formalism.—We consider a system of interacting fermions described by the Hamiltonian:

$$H = \sum_{\mathbf{k},\sigma} \epsilon_{\mathbf{k}\sigma} c^\dagger_{\mathbf{k}\sigma} c_{\mathbf{k}\sigma} + \int d^3\mathbf{r} U(t, \mathbf{r} - \mathbf{r}') c^\dagger_{\mathbf{r}\uparrow} c^\dagger_{\mathbf{r}'\downarrow} c_{\mathbf{r}'\downarrow} c_{\mathbf{r}\uparrow}, \quad (1)$$

where $c^\dagger_\sigma(c_\sigma)$ creates (annihilates) a fermion with spin σ, $\epsilon_k = k^2/2m - \epsilon_F$, where ϵ_F is the Fermi energy, and $U(t, \mathbf{r} - \mathbf{r}')$ is the interatomic interaction being quenched. We describe the short time dynamics of collective modes using the corresponding susceptibility $\chi_{\mathbf{q}}(\omega_{\mathbf{q}}; U_f)$, evaluated with final interactions but initial fermionic configuration [15,16]. In particular, if $\chi_{\mathbf{q}}(\omega_{\mathbf{q}}; U_f)$ has poles at $\omega_{\mathbf{q}} = \Omega_{\mathbf{q}} + i\Delta_{\mathbf{q}}$ in the upper half of the complex plane, then fluctuations that occur after the quench will grow exponentially in time.

Cooperon.—In this section, we obtain the Cooperon, C, i.e., the T matrix that takes into account Pauli blocking of states by the Fermi sea (see Fig. 3). In the center of mass frame in vacuum, the scattering of a pair of particles with identical masses m near a wide Feshbach resonance is described by the T matrix (scattering amplitude) $\tau(E) = \frac{m}{4\pi}(\frac{1}{a} + i\sqrt{mE})^{-1}$, where, E is the energy of the scattered particles and a is the scattering length associated with the pseudopotential $U(\mathbf{r} - \mathbf{r}')$ that appears in Eq. (1). As the Fermi sea breaks translational invariance, we work in the coordinates where the sea is at rest. Comparing the Lippmann-Schwinger equations with and without a Fermi sea (in analogy to Ref. [17]) we obtain

$$C^{-1}(E, \mathbf{q}) = \tau^{-1}(E + 2\epsilon_F - \mathbf{q}^2/4m) + \int \frac{d^3\mathbf{k}}{(2\pi)^3} \frac{n^F(\frac{\mathbf{q}}{2} + \mathbf{k}) + n^F(\frac{\mathbf{q}}{2} - \mathbf{k})}{E - \epsilon_{(\mathbf{q}/2)+\mathbf{k}} - \epsilon_{(\mathbf{q}/2)-\mathbf{k}}}. \quad (2)$$

Here, E and $\mathbf{q}$ are the center of mass frequency and momentum of the pair, and $n^F(\mathbf{k})$ is the Fermi function.

Pairing instability.—The Cooperon is related to the pairing susceptibility via $\chi_{\text{pair}}(\vec{q}) = \int d\vec{k}_1 d\vec{k}_2 G(\vec{k}_1) G(\vec{q} - \vec{k}_1) C(\vec{q}) G(\vec{k}_2) G(\vec{q} - \vec{k}_2)$, where $\vec{q}$ stands for the external frequency and momentum vector $\{E, \mathbf{q}\}$, $d\vec{k}_1$ stands for $d\omega_1 d\mathbf{k}_1/(2\pi)^4$, and $G(\vec{k}_1) = G(\omega_1, \mathbf{k}_1)$ is the bare fermionic Green function in the noninteracting Fermi sea corresponding to the initial state. The pole structure of $\chi_{\text{pair}}(\vec{q})$ match that of $C(\vec{q})$, which we now investigate.

We begin our analysis with the T matrix in vacuum. For each value of a, $\tau(E, \mathbf{q})$ has a line of poles on the BEC side located at $\omega_q = -1/ma^2 + mq^2/4$, corresponding to the binding energy of a Feshbach molecule with center of mass momentum q. As a consequence of energy and momentum conservation the pole frequency is real, indicating that a two-body process in vacuum cannot produce a Feshbach molecule. In the presence of a Fermi sea, the states below the Fermi surface are Pauli blocked, shifting the poles of the Cooperon relative to the T matrix in two ways. First, the real part of the pole Ω_q, which would correspond to the binding energy of a pair in the absence of an imaginary part, uniformly shifts down [see Fig. 2(a)]. This shift indicates the appearance of a paired state on the BCS side as well as stronger binding of the pair on the BEC side. Second, in the range $-\infty < 1/k_Fa \lesssim 1.1$ the pole acquires a positive imaginary part Δ_q that corresponds to the growth rate of the pairing instability. As depicted in Fig. 1, $\Delta_{q=0} \approx 8\epsilon_F e^{\pi/2k_Fa - 2}$ on the BCS side, i.e., the pairing rate matches the BCS gap in equilibrium [18]. On the BEC side, the growth rate continues to increase, reaching a maximum at $k_Fa \approx 2$, and finally decreasing to zero at $k_Fa \approx 1.1$, at which point the Fermi sea can no longer absorb the energy of the Feshbach molecule in a two-body process. Deeper in the BEC regime pairing takes place via the more conventional three-body process and would round the pairing instability curve near $k_Fa \approx 1.1$ in Fig. 1. Pairing at finite q is always slower than at $q = 0$, with Δ_q monotonically decreasing to zero at $q = q_{\text{cut}}$ [see Fig. 2(b)]. Throughout the resonance the approximation $q_{\text{cut}} \approx (\sqrt{3/2})(\Delta_{q=0}/\epsilon_F)k_F$ works reasonably well except in the vicinity of $k_fa \sim 2$ where q_{cut} reaches the maximal value for a two-body process of $2k_f$.

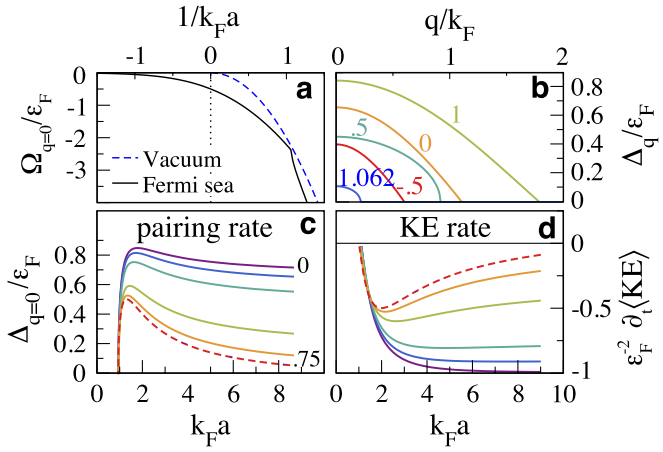

FIG. 2 (color online). Pairing instability. (a) "Binding energy" of a Feshbach molecule in vacuum and in the presence of a Fermi sea (relative to $2\epsilon_F$) as a function of interaction strength, corresponding to the real part of the T matrix pole frequency $\Omega_{q=0} = \mathrm{Re}[\omega_{q=0}]$. The kink occurs when the pair becomes stable. (b) Pairing rate vs momentum for various values of $k_F a$. $q = 0$ is always most unstable wave vector. (c) Pairing rate and (d) rate (in time) of change of kinetic energy vs interaction strength for the BEC side for various temperatures [$T = 0$ (purple, solid), 0.12, 0.22, 0.5, 0.66, $0.75T_F$ (red, dashed)]. Temperature is more effective at suppressing pair production at larger values of $k_f a$ as the binding energy is smaller, thus the peaks in (c) and (d) become sharper at higher temperatures.

Stoner instability.—Our goal is to compute the ferromagnetic susceptibility using the Cooperon to describe effective interatomic interactions, which allows us to include three important aspects of the problem: energy dependence of the scattering amplitude near the Feshbach resonance; Pauli blocking, which renormalizes the energy of the virtual two particle bound states involved in scattering; and Kanamori-like many-body screening [4].

Technically, we compute the vertex function $\Gamma_{\omega,\mathbf{q}}(\omega_1, \mathbf{k}_1)$, which is related to the susceptibility via $\chi_{\mathrm{FM}}(\vec{q}) = \int d\vec{k}_1 G(\vec{q} + \vec{k}_1) G(\vec{k}_1) \Gamma_{\vec{q}}(\vec{k}_1)$. Replacing the point contact interaction vertex by the Cooperon in an RPA type resummation of the vertex function (see Fig. 3 and Ref. [4]) we obtain

$$\Gamma_{\vec{q}}(\vec{k}_1) = 1 + \int d\vec{k}_2 \Gamma_{\vec{q}}(\vec{k}_2) C(\vec{k}_1 + \vec{k}_2 + \vec{q}) G(\vec{k}_2 + \vec{q}) G(\vec{k}_2).$$

To compute the vertex function, a number of approximations are unavoidable. First, we assume that $\mathbf{q}$ and ω are both small, which is valid in the vicinity of the Stoner transition. Second, in the spirit of Fermi liquid theory, we assume that the most important poles come from the Green functions, and hence we replace $G(\mathbf{k}_2 + \mathbf{q}, \omega_2 + \omega) G(\mathbf{k}_2, \omega) \to \frac{2\pi}{v_F} \frac{\mathbf{q}\cdot\mathbf{k}_2}{m\omega - \mathbf{q}\cdot\mathbf{k}_2} \delta(\omega)\delta(|\mathbf{k}_2| - k_F)$ [18]. We then obtain

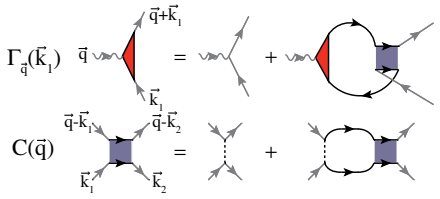

FIG. 3 (color online). Vertex function Γ and Cooperon C: solid lines represent fermions, dashed lines interactions, gray lines external legs, and wavy lines sources.

$$\Gamma_{\mathbf{q},\omega}(\hat{\mathbf{k}}_1) = 1 + \int \frac{d\hat{\mathbf{k}}_2}{4\pi} \Gamma_{\mathbf{q},\omega}(\hat{\mathbf{k}}_2) C(\hat{\mathbf{k}}_1 + \hat{\mathbf{k}}_2, \omega) I_{\mathbf{q},\omega}(\hat{\mathbf{k}}_2), \tag{3}$$

$$I_{\mathbf{q},\omega}(\hat{\mathbf{k}}_2) = \int \frac{k_2^2 dk_2}{2\pi^2} \frac{n_F(\mathbf{k}_2 - \mathbf{q}/2) - n_F(\mathbf{k}_2 + \mathbf{q}/2)}{\omega - \epsilon_{\mathbf{k}_2 - \mathbf{q}/2} + \epsilon_{\mathbf{k}_2 + \mathbf{q}/2}}, \tag{4}$$

and $\hat{\mathbf{k}}$ indicates a vector on the Fermi surface. The approximation involves that we can replace $\mathbf{k}_1$ and $\mathbf{k}_2$, by $\hat{\mathbf{k}}_1$ and $\hat{\mathbf{k}}_2$ when evaluating the Cooperon, i.e., that the Cooperon changes slowly compared to the Green functions. This approximation captures the most singular contributions to the vertex function in the entire parameter range. For weak interactions, where the Cooperon is weakly momentum and frequency dependent, our approximation reduces to the standard RPA [15,18].

In the range $-0.2 \lesssim 1/k_F a \lesssim 1.0$, there is one or more lines of complex poles with a positive imaginary part $\Delta_{\mathbf{q}}$, which corresponds to the Stoner instability in different channels (a combination of momentum and orbital moment). As $q \to 0$, the different instabilities can be identified as different angular momentum channels. In each channel Δ_q grows linearly for small q (as magnetization is a conserved order parameter), saturates at the value $\Delta_{\max}$ at $q_{\max}$, and vanishes for $q > q_{\mathrm{cut}}$ (see Fig. 4).

Discussion.—The growth rates of the pairing instability $\Delta^{\mathrm{BCS}}_{q=0}$ and the ferromagnetic instabilities in the various channels $\Delta^{\mathrm{FM}}_{\max}$ are compared across the Feshbach resonance in Fig. 1. We see that (a) the Cooperon suppresses the growth rate of the ferromagnetic instability but does not eliminate it, (b) the pairing and ferromagnetic instabilities compete over a wide range of interaction strength on both sides of the resonance, and (c) the pairing instability is always dominant. Our results suggest that even if there is a metastable ferromagnetic state [14], it probably cannot be reached dynamically starting from a balanced gas. On short time scales $\sim(\Delta^{\mathrm{FM}}_{\max})^{-1} \sim (\Delta^{\mathrm{BCS}}_{q=0})^{-1}$, both pairing and magnetic correlations develop.

For the finite rate ramp, we should integrate the instantaneous instability rate [15] (i.e., for the order parameter $\Phi_q(t)$ we must solve $\dot{\Phi}_q(t) = \Delta_q(t)\Phi(t)$). As the pairing

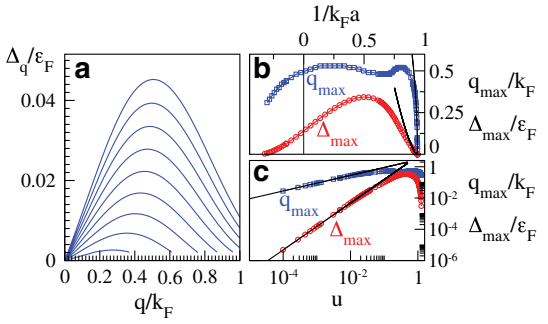

FIG. 4 (color online). Stoner instability. (a) Growth rate of the most unstable mode Δ_q as a function of wave vector q for $T = 0$ and $1/k_F a = 0.85$ (top line), 0.86, 0.87, …, 0.93 (bottom line). (b) The most unstable wave vector $q_{\max}$ (blue) and the corresponding growth rate $\Delta_{\max}$ (red) vs $1/k_F a$. A fit to the mean-field critical theory ($\nu = 1/2$, $z = 3$) is shown with black lines [20]. (c) Details of the critical behavior of $q_{\max}$ and $\Delta_{\max}$ as a function of distance from the transition point $u = (1/k_F a)_c - (1/k_F a)$, $(1/k_F a)_c \approx 0.94$.

instability always dominates the qualitative results will not be affected.

Comparison with experiment.—We underline that the experimentally measured atom loss rate is not the loss rate of atoms out of the trap but instead the loss rate to pair formation. The lack of experimental observation of ferromagnetic domain structures together with the observation of pairing supports our qualitative conclusion that the pairing instability prevails over the Ferromagnetic instability. Quantitatively, the maximum of the pairing instability in the vicinity of $k_F a \approx 2$ but not the onset of the Stoner instability at $k_F a \approx 1$ matches the location of the "transition" found experimentally [11]. The shape of the pairing rate curve [see Fig. 2(c)], especially at higher temperatures, looks qualitatively similar to the atom loss rate found experimentally at lower temperatures [19].

A fast ramp down of the magnetic field was used to convert weakly bound molecules into strongly bound molecules. The kinetic energy of the remaining atoms was measured and showed a minimum at $k_F a \approx 2$ [11], which can be qualitatively understood within our analysis of the pairing instability. The energy of each molecule produced is given by $\sim \mathrm{Re}[\omega_q]$ [see Fig. 2(a)]. The molecular energy corresponds to the kinetic energy of the fermions removed from the Fermi sea, measured with respect to the Fermi energy. Thus the rate of kinetic energy change of "unpaired" atoms is $\sim (\mathrm{Re}[\omega_q] - 2\epsilon_F)\,\mathrm{Im}[\omega_{q=0}]$ [see Fig. 2(d)]. The location of the minimum in the kinetic energy and maximum in the pairing rate agree with Ref. [11].

It is our pleasure to thank E. Altman, A. Chubukov, D. Huse, M. Lukin, S. Stringari, I. Carusotto, A. Georges, and especially G.-B. Jo and W. Ketterle for useful discussions. The authors acknowledge support from a grant from the Army Research Office with funding from the DARPA OLE program, CUA, the Swiss national Science Foundation, NSF Grant No. DMR-07-05472 and PHY-06-53514, AFOSR-MURI, and the Alfred P. Sloan Foundation.

[1] E. Stoner, Philos. Mag. **15**, 1018 (1933).
[2] J. Kanamori, Prog. Theor. Phys. **30**, 275 (1963).
[3] A. Tanaka and H. Tasaki, Phys. Rev. Lett. **98**, 116402 (2007).
[4] L. Chen, C. Bourbonnais, T. Li, and A.-M. S. Tremblay, Phys. Rev. Lett. **66**, 369 (1991).
[5] M. Houbiers *et al.*, Phys. Rev. A **56**, 4864 (1997); Y. Zhang and S. Das Sarma, Phys. Rev. B **72**, 115317 (2005); R. A. Duine and A. H. MacDonald, Phys. Rev. Lett. **95**, 230403 (2005); G. J. Conduit and B. D. Simons, Phys. Rev. A **79**, 053606 (2009); G. J. Conduit, A. G. Green, and B. D. Simons, Phys. Rev. Lett. **103**, 207201 (2009); G. J. Conduit and B. D. Simons, Phys. Rev. Lett. **103**, 200403 (2009); S. Zhang, H.-H. Hung, and C. Wu, Phys. Rev. A **82**, 053618 (2010).
[6] I. Bloch, J. Dalibard, and W. Zwerger, Rev. Mod. Phys. **80**, 885 (2008).
[7] H. J. Miesner *et al.*, Phys. Rev. Lett. **82**, 2228 (1999); H. Schmaljohann *et al.*, Phys. Rev. Lett. **92**, 040402 (2004); L. E. Sadler *et al.*, Nature (London) **443**, 312 (2006).
[8] J. L. Roberts, N. R. Claussen, S. L. Cornish, E. A. Donley, E. A. Cornell, and C. E. Wieman, Phys. Rev. Lett. **86**, 4211 (2001).
[9] M. Greiner, O. Mandel, T. W. Hänsch, and I. Bloch, Nature (London) **419**, 51 (2002).
[10] N. Strohmaier *et al.*, Phys. Rev. Lett. **104**, 080401 (2010).
[11] G.-B. Jo *et al.*, Science **325**, 1521 (2009).
[12] L. J. LeBlanc, J. H. Thywissen, A. A. Burkov, and A. Paramekanti, Phys. Rev. A **80**, 013607 (2009).
[13] W. Ketterle and M. W. Zwierlein, in *Proceedings of the International School of Physics "Enrico Fermi", Course CLXIV, Varenna, June 2006*, edited by M. Inguscio, W. Ketterle, and C. Salomon (IOS Press, Amsterdam, 2008), p. 20.
[14] S. Pilati, G. Bertaina, S. Giorgini, and M. Troyer, Phys. Rev. Lett. **105**, 030405 (2010); S.-Y. Chang, M. Randeria, and N. Trivedi, Proc. Natl. Acad. Sci. U.S.A. **108**, 51 (2010).
[15] M. Babadi, D. Pekker, R. Sensarma, A. Georges, and E. Demler, arXiv:0908.3483.
[16] A. Lamacraft and F. M. Marchetti, Phys. Rev. B **77**, 014511 (2008).
[17] N. V. Prokof'ev and B. V. Svistunov, Phys. Rev. B **77**, 125101 (2008).
[18] A. A. Abrikosov, L. P. Gorkov, and I. E. Dzyaloshinski, *Methods of Quantum Field Theory in Statistical Physics* (Dover Publications, New York, 1975).
[19] We speculate that the mismatch between the computed and observed temperature dependence of the pairing rate has to do with the nonlinear dynamics that follow the initial instability.
[20] H. V. Lohneysen, A. Rosch, M. Vojta, and P. Wolfle, Rev. Mod. Phys. **79**, 1015 (2007).